Available online at www.sciencedirect.com

SciVerse ScienceDirect

Ceramics International 38 (2012) 5791–5797

CERAMICS INTERNATIONAL

www.elsevier.com/locate/ceramint

Synthesis and investigation of TiO_2 nanotube arrays prepared by anodization and their photocatalytic activity

Hailei Li, Lixin Cao *, Wei Liu, Ge Su, Bohua Dong

Institute of Materials Science and Engineering, Ocean University of China, Songling Road 238, Qingdao 266100, Shandong Province, PR China

Received 23 March 2012; received in revised form 8 April 2012; accepted 9 April 2012
Available online 14 April 2012

Abstract

TiO_2 nanotube arrays were successfully prepared by anodic oxidation method in the electrolyte of ethylene glycol and deionized water mixed in 9:1 volumetric ration including 0.5 wt.% NH_4F. The microstructure and phase compositions of samples annealing from 0 °C to 800 °C were characterized by field-emission scanning electron microscope (FESEM) and X-ray diffraction (XRD). FESEM showed that the obtained nanotubes with diameter 80–100 nm and length 4.89 μm were highly ordered and perpendicular to Ti substrate. The tubular structure collapsed at 680 °C. The photocatalytic activity of samples annealing at different temperature were calculated by the degradation of a model dye, methyl orange (MO), under UV light illumination. The results indicated the phase composition and the morphology of TiO_2 nanotubes both played an important role in the degradation of MO. In addition, the effects of initial solution pH and dye concentration on degradation of MO had also been investigated. As a result, the optimum values of calcination temperature, initial solution pH and dye concentration were found to be 550 °C, 3, 10 mg/l, respectively. The best photodegradation of MO was 76% under illumination for 3 h.

Keywords: TiO_2 nanotube arrays; Anodic oxidation; Photocatalytic reaction; Methyl orange

1. Introduction

As an important inorganic functional material, TiO_2 has been widely used in applications of dye-sensitized solar cells (DSSC), environmental purification, water splitting, gas sensor bio-application, optical and photonic [1–10] due to its excellent dielectric effect, photoelectric conversion and superior photocatalytic properties. In the past few years, TiO_2 nanoparticles as traditional photocatalyst have been used to photodegradate the organic pollutants. But to overcome their some drawbacks of low surface area, easy aggregation during reaction and difficult separation after reaction, high recombination efficiency of photogenerated electron–hole pairs, several methods for fabricating the fixed TiO_2 photocatalyst on solid support substrates have been studied, including sol–gel method [11], laser calcination [12], template synthesis [13], sputtering [14] and anodic oxidation [15]. Among these preparations, highly ordered TiO_2 nanotube arrays growing directly on Ti substrate are fabricated by anodic oxidation which is simplicity in operation and easy control in the synthesis.

Zwilling et al. [16] first fabricated TiO_2 in the form of hollow nanotubes on titanium alloy by anodic oxidation method, and in 2001, G.K. Mor et al. [17] reported that the uniform TiO_2 nanotube arrays were synthesized on a pure titanium sheet using the same method. Following then, preparation parameters influencing on the structure of TiO_2 nanotube arrays had been reported. These various parameters concluded electrolyte composition, the anodic voltage, time and pH. Furthermore, attention also had been paid to the effect of TiO_2 nanotubes structure and phase composition on photodegradation of pollutants. However, the results were not consistent with each other. For example, Liang and Li [18] reported that TiO_2 nanotubes with a mixed phase of anatase/rutile had a better photocatalytic activity. Whereas, Fang et al. [19] claimed that TiO_2 nanotubes with a pure anatase phase obtained a better photocatalytic activity. Therefore, it is still worthy of paying attention to improvement of photocatalytic activity of TiO_2 nanotube arrays.

In this paper, the aim of our study was focused on the photocatalytic activity of TiO_2 nanotube arrays fabricated by

* Corresponding author. Tel.: +86 532 66781901; fax: +86 532 66781320.
E-mail address: caolixin@mail.ouc.edu.cn (L. Cao).

0272-8842/$36.00 © 2012 Published by Elsevier Ltd and Techna Group S.r.l.
http://dx.doi.org/10.1016/j.ceramint.2012.04.026

anodic oxidation method. Methyl orange (MO) was used as a model dye. The influences of experimental variables, including calcination temperature, initial pH and dye concentration, had been detailed and systematically investigated.

2. Experimental

2.1. Materials

Titanium foils (10 mm × 15 mm size, 0.89 mm thickness, 99.7% purity) were mechanically polished by different abrasive papers (400#, 600#, 1000#, 1200#), then followed by sonicating in acetone, ethanol and deionized water for 30 min, respectively. The titanium was chemically etched in acidic mixture solution of $HF:HNO_3:H_2O$ ($HF/HNO_3/H_2O$ = 1:4:5, v/v/v) for 30 s to form a fresh smooth surface. Finally, the titanium was washed with deionized water and then dried at room temperature in air. All the other chemicals were of analytical grade and used as received without further purification.

2.2. Preparation of TiO_2 nanotube arrays

Anodization experiments were performed in a two-electrodes configuration with Ti foil (oxidation area 1 cm × 1 cm) as the anode and graphite foil as the counter electrode, respectively. Both electrodes were immersed in 100 ml organic electrolyte containing 0.5 wt.% NH_4F, 10 vol.% H_2O and 90 vol.% ethylene glycol (EG). The whole oxidation process was followed as: (1) a potential of 30 V was applied by a DC power source; (2) the voltage increased to 30 V with a rate of 1 V min^{-1} and was kept at 30 V for 1 h; (3) the distance between the two electrodes was fixed at 4 cm; (4) the electrochemical experimentals was carried out at 30 °C and the electrolyte was kept uniform by continuously stirred. Finally, the fabricated TiO_2 nanotube arrays were annealed in muffle furnace for 2 h with heating rate of 3 °C/min and cooling to room temperature.

2.3. Photocatalytic activity measurements

Photocatalytic experiments were carried out by immersing TiO_2 nanotube arrays (1 cm × 1 cm) in 20 ml quartz glass with 10 ml model dye, methyl orange (MO) solution. A 300 W high pressure mercury lamp was used as light source. Prior to irradiation, TiO_2 nanotube arrays were soaked in MO solution for 30 min in a dark environment to achieve the equilibrium of adsorption and desorption. The solution was stirred with a magnetic agitator in all the runs. The distance between TiO_2 nanotube arrays film and light source was 12 cm. The absorbance changes of MO were measured using a UV spectrophotometer at different time intervals (30 min) during the whole photodegradation process. Fig. 1 showed the reactor.

2.4. Characterization techniques

The surface morphologies of obtained samples were observed using field-emission scanning electron microscope (FE-SEM, Hitachi S-4800), and their crystalline phase was characterized by X-ray diffraction diffractometer (XRD, Bruker D8 ADVANCE, Cu Kα radiation). The photocatalytic activity of TiO_2 nanotube arrays was represented by the degradation of MO under UV light illumination. UV-vis spectrophotometer (岛津, UV-2550) with wavelength range of 200–700 nm was used to test the absorption spectra of MO, the absorbance of MO was taken at the maximum absorbed

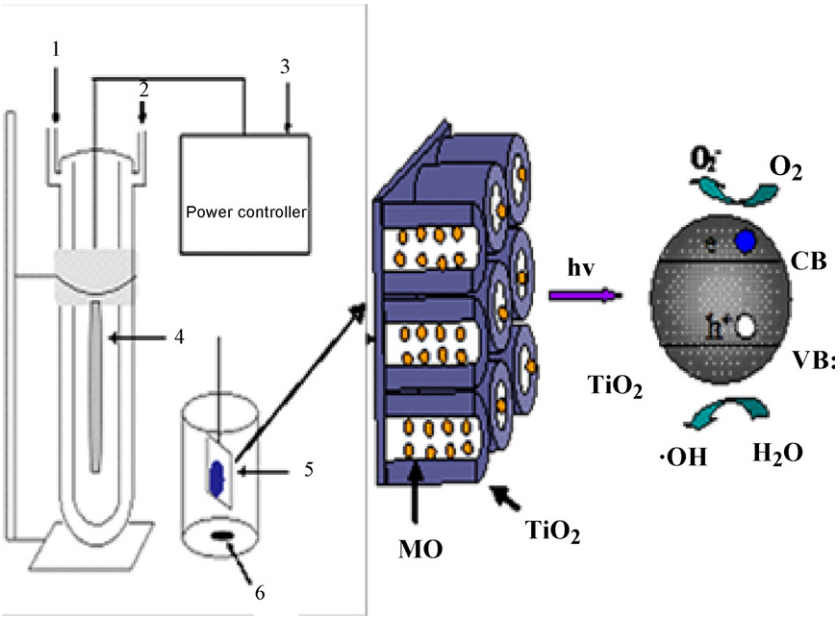

Fig. 1. Schematic graph of photocatalytic reactor. (1) Inlet of cooling water; (2) outlet of cooling water; (3) power controller; (4) UV lamp; (5) TiO_2 nanotube arrays; (6) magnetic stirrer.

wavelength. The photodegradation ratio of MO (η) was calculated using the following formula:

$$\eta = \left[\frac{A_0 - A}{A_0}\right] \times 100\%$$

where A_0, the original absorbance of methyl orange solution; A, the absorbance of methyl orange at time t.

3. Results and discussion

3.1. Characteristics of TiO_2 nanotube arrays

Fig. 2 showed the different XRD patterns of the TiO_2 nanotube arrays with calcination temperatures varying from 0 to 800 °C. The results exhibited that the crystalline phase of the samples depended on the heat treatment temperature. As expected, pattern a only showed peaks of Ti substrate, indicating the dominant phase of TiO_2 nanotube arrays without calcination was amorphous. In contrast, patterns b–f showed the crystalline phase of nanotubes calcined at 300, 450, 550, 680 and 800 °C, respectively. It was noted that anatase or rutile phase was observed with the calcination temperature increasing and the phase ratios of anatase/rutile were different when the samples were calcinated at different temperatures. Pattern b showed nanotubes possessed anatase structure at $2\theta = 25.2^\circ$ (1 0 1), 37.8° (0 0 5), 48° (2 0 0) and 53.8° (1 0 5) (PDF#21-1272, JCPDS), respectively, and no rutile structure was detected. Increasing the annealing temperature, the crystallinity of anatase phase increased, a small fraction of rutile phase appeared at $2\theta = 27.5^\circ$ at the same time shown in pattern d. Moreover, patterns d–f showed that the intensities of rutile peaks became stronger while that of anatase peaks became weaker along with the calcination temperature elevating. It was conformed that at 800 °C (pattern f), the anatase peak at $2\theta = 25.2^\circ$ and 48° disappeared completely and the rutile peaks became stronger. Based on the fact that rutile phase possessed better stability than anatase phase, it was inferred that the phase transformation from anatase to rutile occurred at high calcination temperature. It had to be noted that the intensities of Ti peaks corresponding to 38.4° (0 0 2), 40.4° (1 0 1), 53.2° (1 0 2) and 63.2° (1 1 0) became weaker or even disappeared gradually, indicating that the remaining Ti substrate was oxidated by O_2 during heat treatment process.

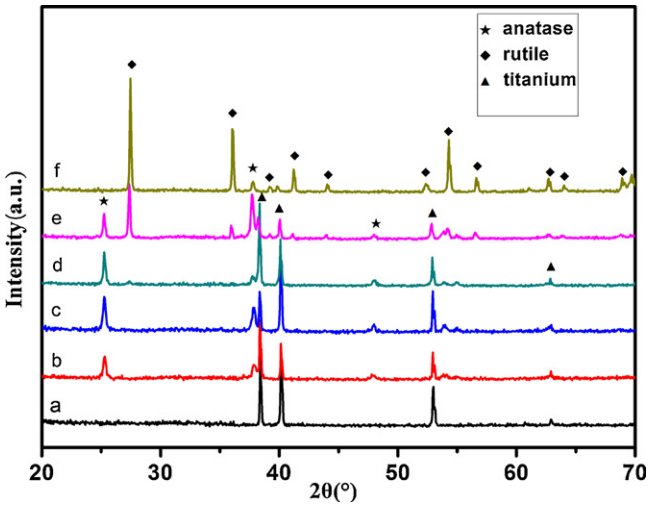

Fig. 2. XRD patterns of TiO_2 nanotube arrays: (a) without calcination; (b) 300 °C; (c) 450 °C; (d) 550 °C; (e) 680 °C; (f) 800 °C.

3.2. Surface morphology of TiO_2 nanotube arrays

In order to investigate the effect of calcination temperature on the surface morphologies of the TiO_2 nanotube arrays, Fig. 3 presents FESEM images of samples annealing from 0 °C to 800 °C. Fig. 3a showed the as-prepared nanotubes were more uniform, highly ordered over the whole Ti substrate, the average inner diameter and the tube length of TiO_2 nanotubes were approximately 80–100 nm and 4.89 μm, respectively. Fig. 3b–d showed the morphology structure of the samples annealing from 300 °C to 550 °C were not significantly altered. However, increasing the calcination temperature upon to 680 °C, the nanotube structure was completely destroyed, and the grain size grew larger at 800 °C, indicating the heat treatment accelerate the grain growth of TiO_2. This result is consistent with that reported by S. Sreekantan [20].

3.3. Photocatalytic activity

3.3.1. Effect of heat treatment of catalyst

Experiments about the effect of calcination temperature on the photocatalytic activity of TiO_2 nanotube arrays were evaluated by photodegradation of MO under UV illumination for 4 h. Fig. 4 demonstrated the MO degradation efficiency with the TiO_2 photocatalyst annealing from 0 °C to 800 °C. It was clearly shown that TiO_2 nanotubes without calcination had no significant photocatalytic activity. When the calcination temperature of photocatalyst increased, the photodegradation rate of MO obviously enhanced, and the highest photodegradation rate was achieved at 550 °C. Oppositely, the photodegradation efficiency reduced with the further calcination temperature increasing.

It is noted that the photodegradation efficiency of organic pollutants agrees with a pseudo-first-order kinetic model [21] by the linear relationship $\ln[C_0/C_t]=\kappa t$, the kinetic constant (κ) and regression coefficients (R^2) were shown in Table 1, it was obvious that kinetic constant (κ) calculated at 550 °C was the largest. That is to say, the TiO_2 nanotube arrays annealing at 550 °C possessed the optimal photocatalytic performance. The result may be ascribed to the optimum composition of anatase and rutile phase and well tubular structure of TiO_2, contributing to larger surface area and much efficiency separation of photogenerated electron–hole pairs. Some other researchers [22–24] also had demonstrated that the mixed phases of TiO_2 nanotubes dominantly influenced photodegradation efficiency of MO and provided details of the mixed phased on the photoactivity of TiO_2.

3.3.2. Effect of pH

As the pH values of the dyestuff waste could be different in practical application, additional experiments were carried out

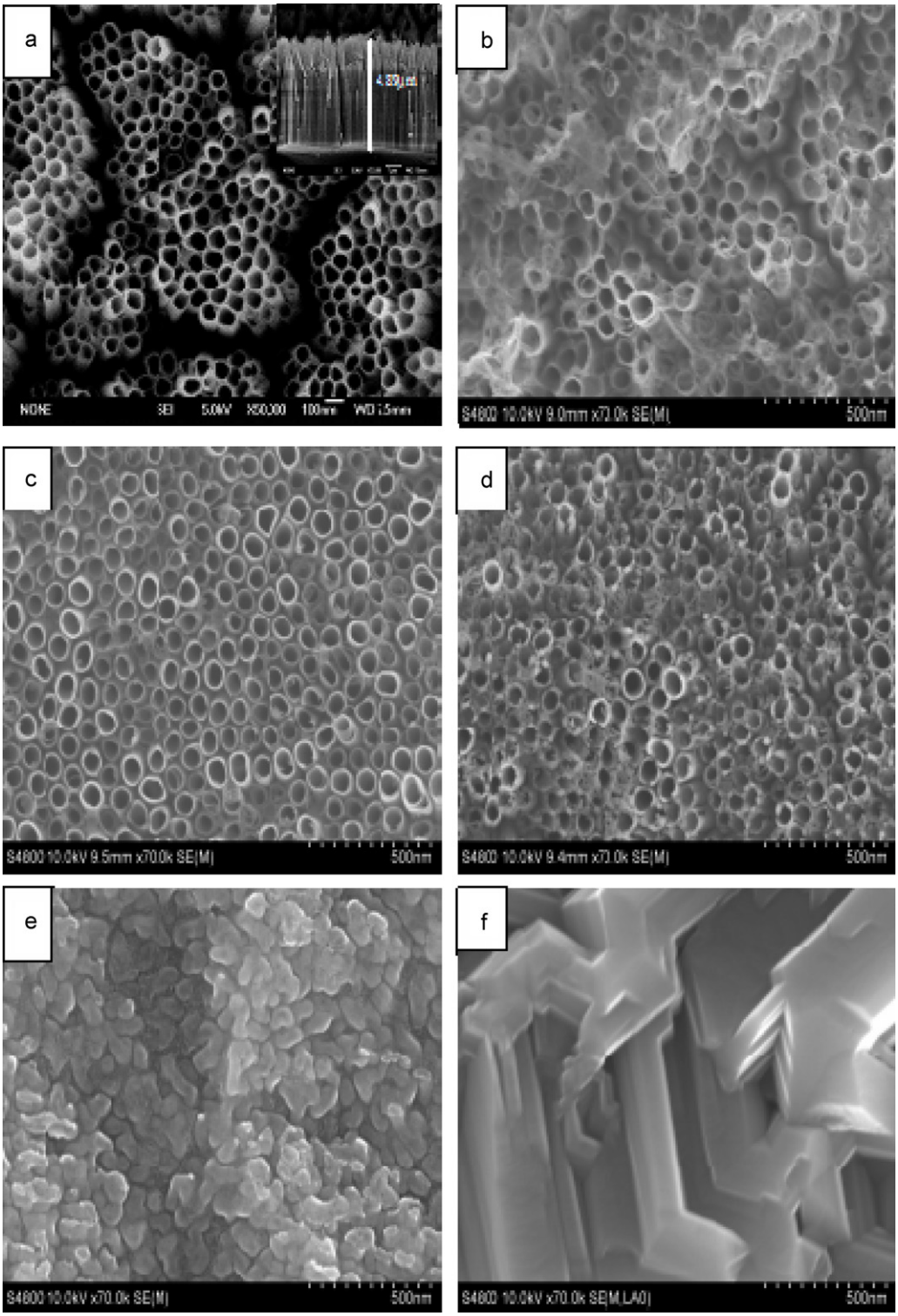

Fig. 3. FESEM images of TiO_2 annealing at different temperature for 2 h. (a) As-prepared sample; (b) 300 °C; (c) 450 °C; (d) 550 °C; (e) 680 °C; (f) 800 °C.

Table 1
The kinetic constant and regression coefficients of MO degradation by TiO_2 nanotube arrays with different calcination temperature.

T (°C)	0	300	450	550	680	800
K (min^{-1})	0.00007	0.00049	0.00176	0.00224	0.00058	0.00040
R^2	0.9698	0.9915	0.9947	0.9981	0.9903	0.9962

to examine the effect of initial pH values of MO solution on the photocatalytic reaction. The catalyst was annealed at 550 °C. The initial pH values of the test solution were manually adjusted from 1.0 to 12.0 with 1 mol l^{-1} H_2SO_4 or 1 mol l^{-1} NaOH without any modification during UV irradiation. All the other experimental conditions were identical. Fig. 5 demonstrated the photodegradation efficiency of MO at different pH

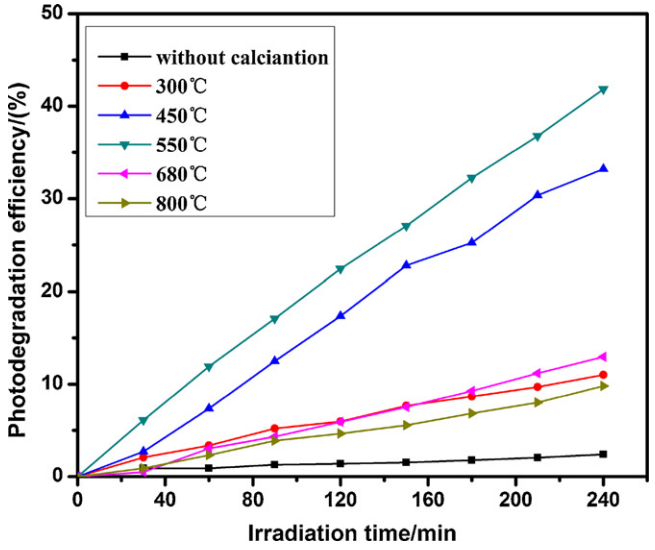

Fig. 4. Effects of calcination temperature on photodegradation efficiency of methyl orange (MO) under UV illumination for 4 h (C_{MO} = 10 mg/l, V_{MO} = 10 ml).

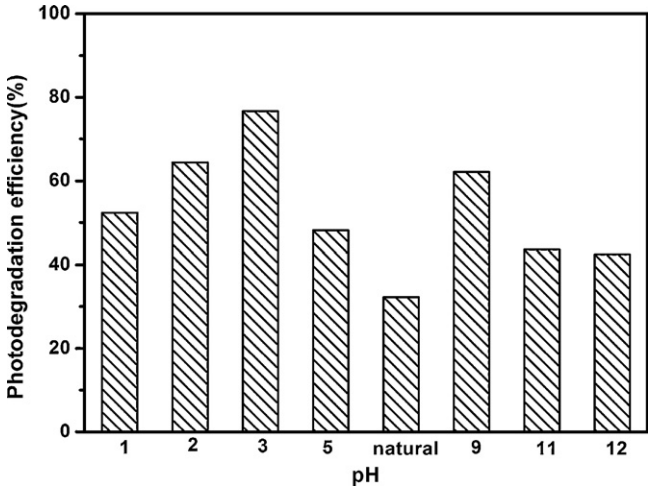

Fig. 5. Effects of initial pH on photodegradation efficiency of methyl orange (MO) under UV illumination for 3 h (C_{MO} = 10 mg/l, V_{MO} = 10 ml).

values of solution. These figures indicated the photodegradation efficiencies changed sharply with initial pH value and were both enhanced relatively in acidic or alkaline solution compared with natural pH of MO solution. The maximum photodegradation efficiency was observed at pH 3 and 76% was reached after illumination for 180 min. Other studies about the effects of solution pH on photodegradation had been performed [25–29], and the conclusions were the same as the results in this paper. The reason that the photodegradation efficiency of MO depended on solution pH was due to the competitive factors including catalyst surface charge, the absorption/desorption of MO on TiO_2 surface, and the oxidation potential of TiO_2 valence band [30]. It was well known to us that the charges on TiO_2 surface was different on the basis of the zero-point charge (zpc) of TiO_2, and the zpc value for TiO_2 ranges from 6 to 7 [31]. In acidic solution, the photodegradation efficiency increased first and then decreased with the pH value decreasing. The maximum photodegradation efficiency arrived at pH 3. For $pH < pH_{zpc}$, TiO_2 was positively charged and absorbed MO molecules by electrostatic attraction. But for solution $pH < 3$, H^+ ions competed with OH^- and occupied the active sites of TiO_2 surface. Hence the amount of hydroxyl radicals ($^{\bullet}OH$) was reduced. In alkaline solution, the photodegradation efficiency increased first and then decreased with the pH value increasing. The maximum photodegradation efficiency arrived at pH 9. For $pH > pH_{zpc}$, TiO_2 was negatively charged and the absorption of MO molecules became weaker due to repulsive forces, but the hydroxyl radicals were produced ($OH^- + h^+ \rightarrow {}^{\bullet}OH$) and could reacted rapidly with MO molecules. However, for solution $pH > 9$, the amount of photogenerated holes reduced due to the shift of the reduction valence band. As a result, hydroxyl radicals ($^{\bullet}OH$) were gradually overwhelmed. It was worthwhile to mention that the solution condition with pH values less than 3 or higher than 9 did not favor the photodegradation rate of MO.

3.3.3. Effect of dye concentration

The effect of initial dye concentration on photodegradation of MO had been performed in this experiment. The catalyst was annealed at 550 °C. The initial concentration of MO varied from 5 to 40 mg/l and all solution were kept at natural pH. The results were showed in Fig. 6. It could be seen that the removal efficiency of MO decreased from 59.3% to 14% as the initial MO concentration increased from 5 to 40 mg/l. When the other factors were under the same condition, it was clear that photocatalytic degradation of MO decreased with the dye concentration increasing.

As we all know, the photogenerated holes migrated onto the tubes surface and reacted with absorbed OH^-, the production of which were hydroxyl radicals ($OH^{\bullet}$). Strong evidence suggested that the photocatalytic degradation of aromatic compounds was oxidized by hydroxylation ($OH^- + h^+ \rightarrow {}^{\bullet}OH$) [32]. In another word, the generation of $OH^{\bullet}$ radicals could

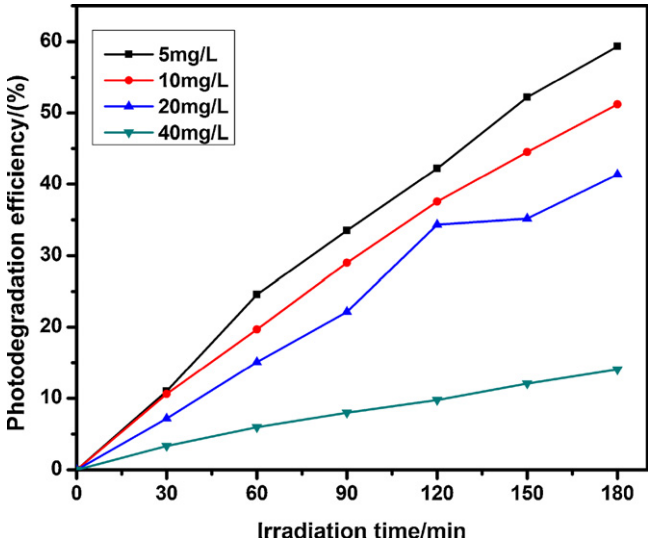

Fig. 6. Effects of initial concentration solution on photodegradation efficiency of methyl orange (MO) under UV illumination for 3 h (V_{MO} = 10 ml, natural pH).

diminish the recombination rate of photogenerated electron–hole pairs. Okamoto et al. [33,34] also pointed out that the formation of $OH^{\bullet}$ radicals should be the rate-determining step of photodegradation reaction due to their direct reaction with aromatic compounds. So the more OH^- absorbed on the tubes surface, the more amount of $OH^{\bullet}$ radicals would generate. Thus, at a low initial dye concentration, much OH^- absorbed on the TiO_2 nanotube surface and formed $OH^{\bullet}$ radicals. As a result, the photodegradation efficiency of MO was high. At higher initial dye concentration, the dye competing with OH^- absorbed on the active sites of TiO_2 nanotube surface and the number of $OH^{\bullet}$ radicals reduced, so the degradation efficiency decreased.

4. Conclusions

In summary, TiO_2 nanotube arrays were fabricated on Ti substrate by anodization method in ethylene glycol (EG) electrolyte. The morphology and microstructure of obtained TiO_2 nanotube were characterized by FESEM and XRD. FESEM showed that the obtained nanotubes were well organized and uniform arrays. The average inner diameter and the tube length of TiO_2 nanotubes were approximately 80–100 nm and 4.89 μm, respectively. Furthermore, photocatalytic activity of TiO_2 nanotube arrays was also studied experimentally. The variables influencing the photodegradation of MO under UV illumination included nanotubes calcination temperature, initial pH, and dye concentration. The results exhibited that calcination temperature of TiO_2 nanotube arrays was an important parameter for photocatalytic activity. TiO_2 nanotube arrays annealing at 550 °C possessed anatase phase with a tiny rutile phase, and TiO_2 still maintain the well tubular structure. As a result, the highest photodegradation rate of MO reached 41.8%. In addition, the degradation rate of MO was enhanced in both acidic and alkaline solution and the best condition of pH was 3. Moreover, the MO removal decreased with dye concentration increasing.

Acknowledgements

The authors thank the National Science Foundation of China (NSFC 50672089, 51172218), Program for New Century Excellent Talents in University (NCET-08-0511) and Promotive Research Fund for Young and Middle-aged Scientists of Shandong Province (BS2010CL049) for financial support.

References

[1] Q.W. Chen, D.S. Xu, Large-scale, noncurling, and free-standing crystallized TiO_2 nanotube arrays for dye-sensitized solar cells, Journal of Physical Chemistry C 113 (2009) 6310–6314.
[2] K.T. Ranjit, I. Willner, S. Bossmann, A. Braun, Iron(III) phthalocyanine-modified titanium dioxide: a novel photocatalyst for the enhanced photodegradation of organic pollutants, Journal of Physical Chemistry B 102 (1998) 9397–9403.
[3] M. Hepel, I. Kumarihamy, C.J. Zhong, Nanoporous TiO_2-supported bimetallic catalysts for methanol oxidation in acidic media, Electrochemistry Communications 8 (2006) 1439–1444.
[4] H. Yamashita, Y. Ichihashi, S.G. Zhang, T. Tatsumi, M. Anpo, Photocatalytic decomposition of NO at 275 K on titanium oxide catalysts anchored within zeolite cavities and framework, Applied Surface Science 121/122 (1997) 305–309.
[5] Y.F. Zhu, J.J. Shi, Z.Y. Zhang, Development of a gas sensor utilizing chemiluminescence on nanosized titanium dioxide, Analytical Chemistry 74 (2001) 120–124.
[6] G.K. Mor, K. Shankar, M. Paulose, Enhanced photocleavage of water using titania nanotube arrays, Nano Letters 5 (2005) 191–195.
[7] J.H. Park, S. Kim, A.J. Bard, Novel carbon-doped TiO_2 nanotube arrays with high aspect ratios for efficient solar water splitting, Nano Letters 6 (2006) 24–28.
[8] M. Enachi, M. Stevens-Kalceff, L. Tiginyanu, Cathodoluminescence of TiO_2 nanotubes prepared by low-temperature anodization of Ti foils, Materials Letters 64 (2010) 2155–2158.
[9] V.V. Sergentu, I.M. Tiginyanu, V.V. Ursaki, Prediction of negative index material lenses based on metallo-dielectric nanotubes, Physica Status Solidi (RRL) 2 (2008) 242–244.
[10] M. Enachi, L. Tiginyanu, V. Sprincean, Self-organized nucleation layer for the formation of ordered arrays of double-walled TiO_2 nanotubes with temperature controlled inner diameter, Physica Status Solidi (RRL) 4 (2010) 100–102.
[11] T.A. Egerton, M. Janus, A.W. Morawski, New TiO_2/C sol–gel electrodes for photoelectrocatalytic degradation of sodium oxalate, Chemosphere 63 (2006) 1203–1208.
[12] J.Q. Li, L.P. Li, L. Zheng, Photoelectrocatalytic degradation of rhodamine B using Ti/TiO_2 electrode prepared by laser calcination method, Electrochimica Acta 51 (2006) 4942–4949.
[13] B.B. Lakshmi, C.J. Patrissi, C.R. Martin, Sol–gel template synthesis of semiconductor oxide micro- and nanostructures, Chemistry of Materials 9 (1997) 2544–2550.
[14] C. He, X.Z. Li, N. Graham, Preparation of TiO_2/ITO and TiO_2/Ti photoelectrodes by magnetron sputtering for photocatalytic application, Applied Catalysis A: General 305 (2006) 54–63.
[15] G.K. Mor, O.K. Varghese, M. Paulose, Transparent highly ordered TiO_2 nanotube arrays via anodization of titanium thin films, Advanced Functional Materials 15 (2005) 1296–1297.
[16] V. Zwilling, E. Darque-Ceretti, A. Boutry-Forveille, Structure and physicochemistry of anodic oxide films on titanium and TA6V alloy, Surface and Interface Analysis 27 (1999) 629–637.
[17] G.K. Mor, O.K. Varghese, M. Paulose, Fabrication of tapered, conical-shaped titania nanotubes, Journal of Materials Research 18 (2003) 2588–2593.
[18] H.C. Liang, X.Z. Li, Effects of structure of anodic TiO_2 nanotube arrays on photocatalytic activity for the degradation of 2,3-dichlorophenol in aqueous solution, Journal of Hazardous Materials 162 (2009) 1415–1422.
[19] D. Fang, Z.P. Luo, K.L. Huang, Effect of heat treatment on morphology, crystalline structure and photocatalysis properties of TiO_2 nanotubes on Ti substrate and freestanding membrane, Applied Surface Science 257 (2011) 6451–6461.
[20] S. Sreekantan, R. Hazan, Z. Lockman, Photoactivity of anatase-rutile TiO_2 nanotubes formed by anodization method, Thin Solid Films 518 (2009) 16–21.
[21] K. Nagaveni, G. Sivalingam, M.S. Hedge, Solar photocatalytic degradation of dyes: high activity of combustion synthesized nano TiO_2, Applied Catalysis B: Environmental 48 (2004) 83–93.
[22] P. Xiao, D.W. Liu, B.B. Garcia, Electrochemical and photoelectrical properties of titania nanotube arrays annealed in different gases, Sensors and Actuators B: Chemical 134 (2008) 367–372.
[23] V.K. Mahajan, M. Misra, K.S. Raja, Selforganized TiO_2 nanotubular arrays for photoelectrochemical hydrogen generation: effect of crystallization and defect structures, Journal of Physics D: Applied Physics 41 (2008) 125307.
[24] H.Y. Chang, W.J. Tzeng, S.Y. Cheng, Modification of TiO_2 nanotube arrays by solution coating, Solid State Ionics 180 (2009) 817–821.
[25] L.B. Reutergardh, M. angphasuk, Photocatalytic decolourization of reactive azo dye: a comparison between TiO_2 and CdS photocatalysis, Chemosphere 35 (1997) 585–596.

[26] S. Al-Quadawi, S.R. Salman, Photocatalytic degradation of methyl orange as a model compound, Journal of Photochemistry and Photobiology A 148 (2002) 161–168.
[27] K.M. Parida, N. Sahu, N.R. Biswal, Preparation, characterization, and photocatalytic activity of sulfate-modified titania for degradation of methyl orange under visible light, Journal of Colloid and Interface Science 318 (2008) 231–237.
[28] J.H. Li, C.L. Mi, J. Li, The removal of MO molecules from aqueous solution by the combination of ultrasound/adsorption/photocatalysis, Ultrasonics Sonochemistry 15 (2008) 949–954.
[29] M.R. Sohrabi, M. Ghavami, Photocatalytic degradation of Direct Red 23 dye using UV/TiO_2: effect of operational parameters, Journal of Hazardous Materials 153 (2008) 1235–1239.
[30] M.V. Shankar, S. Anandan, N. Venkatachalam, Novel thin-film reactor for photocatalytic degradation of pesticides in an aqueous solutions, Journal of Chemical Technology and Biotechnology 79 (2004) 1279–1285.
[31] K.E. O'Shea, E. Pernas, J. Saiers, The influence of mineralization products on the coagulation of TiO_2 photocatalyst, Langmuir 15 (1999) 2071–2076.
[32] Y.W. Tsong, C.W. Chi, Heterogeneous photocatalytic oxidation of phenol with titanium dioxide powders, Industrial & Engineering Chemistry Research 30 (1991) 1293–1300.
[33] K. Okamoto, Y. Yamamoto, H.T. Anaka, Heterogeneous photocatalytic decomposition of phenol over TiO_2 powder, Bulletin of the Chemical Society of Japan 58 (1985) 2015–2022.
[34] K. Okamoto, Y. Yamamoto, H. Tanaka, Kinetics of heterogeneous photocatalytic decomposition of phenol over anatase TiO_2 powder, Bulletin of the Chemical Society of Japan 58 (1985) 2023–2028.